Photosystem II and Pigment Dynamics among Ecotypes of the Green Alga *Ostreococcus*[1]

Christophe Six[2]*, Ryan Sherrard, Marie Lionard, Suzanne Roy, and Douglas A. Campbell

Biology Department, Mount Allison University, Sackville, New Brunswick, Canada E4L 1G7 (C.S., R.S., D.A.C.); and Institut des Sciences de la Mer, Université du Québec à Rimouski, Rimouski, Quebec, Canada G5L 3A1 (M.L., S.R.)

We investigated the photophysiological responses of three ecotypes of the picophytoplankter *Ostreococcus* and a larger prasinophyte *Pyramimonas obovata* to a sudden increase in light irradiance. The deepwater *Ostreococcus* sp. RCC809 showed very high susceptibility to primary photoinactivation, likely a consequence of high oxidative stress, which may relate to the recently noted plastid terminal oxidase activity in this strain. The three *Ostreococcus* ecotypes were all capable of deploying modulation of the photosystem II repair cycle in order to cope with the light increase, but the effective clearance of photoinactivated D1 protein appeared to be slower in the deepwater *Ostreococcus* sp. RCC809, suggesting that this step is rate limiting in the photosystem II repair cycle in this strain. Moreover, the deepwater *Ostreococcus* accumulated lutein and showed substantial use of the xanthophyll cycle under light stress, demonstrating its high sensitivity to light fluctuations. The sustained component of the nonphotochemical quenching of fluorescence correlated well with the xanthophyll deepoxidation activity. Comparisons with the larger prasinophyte *P. obovata* suggest that the photophysiology of *Ostreococcus* ecotypes requires high photosystem II repair rates to counter a high susceptibility to photoinactivation, consistent with low pigment package effects in their minute-sized cells.

The prasinophytes are marine planktonic green algae with a phylogenetic position branching near the base of the green lineage (Baldauf, 2003; Turmel et al., 2009). They are widespread in temperate (Diez et al., 2001; Zhu et al., 2005) and polar (Lovejoy et al., 2007) marine habitats, in which they are often significant contributors to primary production (Not et al., 2004). The prasinophytes include the smallest known eukaryotic photoautotroph, *Ostreococcus tauri* (Courties et al., 1994; Chrétiennot-Dinet et al., 1995), whose particularly simple structure makes it an attractive model minimal chlorophyte, and indeed, minimal eukaryote (Derelle et al., 2006). Recently, genomic sequences for three *Ostreococcus* strains, isolated from different ecological niches, have become available (Derelle et al., 2006; Palenik et al., 2007), thus increasing the interest of these models for understanding acclimation processes in this deep-branching group of chlorophytes.

Photoacclimation strategies differ in two *Ostreococcus* strains (Cardol et al., 2008; Six et al., 2008), which, although belonging to different phylogenetic clades, are nonetheless morphologically indistinguishable (Rodríguez et al., 2005). *O. tauri*, a eutrophilic lagoon species, modulates PSII content to enable acclimation and growth over a wide range of irradiances. In marked contrast, *Ostreococcus* sp. (*O.* sp.) RCC809, isolated at 105 m depth in the tropical Atlantic Ocean, modulates the size of its large PSII antenna in a strategy that accommodates a narrower range of light levels but that incurs lower nutrient costs compared with photoacclimation in *O. tauri* (Six et al., 2008). The evidence for different light acclimation strategies between these two *Ostreococcus* ecotypes raises the question of the underlying physiological processes for niche adaptation in these closely related organisms. Cardol et al. (2008) recently analyzed the coastal *O. tauri* and the deepwater *O.* sp. RCC809 grown under low to moderate light and found exciting evidence for a plastid terminal oxidase electron flow path in *O.* sp. RCC809 from PSII back to oxygen, short-circuiting the usual Z scheme in a mechanism to generate a transthylakoidal pH gradient without net generation of reductant. Like all oxygenic photoautotrophs, the prasinophytes suffer photoinactivation of PSII (Aro et al., 1993; Tyystjarvi, 2008; Guskov et al., 2009) at a rate approximately proportional to the incident irradiance (Nagy et al., 1995; Hakala et al., 2005). To counter this photoinactivation, a PSII repair cycle proteolytically removes the photoinactivated D1 protein (Silva et al., 2003) and replaces it through de novo

[1] This work was supported by the Natural Sciences and Engineering Research Council of Canada Canada Foundation for Innovation.

[2] Present address: Marine Photosynthetic Prokaryotes Group, UMR 7144 Université Pierre et Marie Curie (Paris 6) and CNRS, Station Biologique de Roscoff, 29682 Roscoff, France.

* Corresponding author; e-mail six@sb-roscoff.fr.

The author responsible for distribution of materials integral to the findings presented in this article in accordance with the policy described in the Instructions for Authors (www.plantphysiol.org) is: Christophe Six (six@sb-roscoff.fr).

www.plantphysiol.org/cgi/doi/10.1104/pp.109.140566

synthesis and reassembly with the remaining subunits (Aro et al., 1993). If photoinactivation outruns the rate of repair, the PSII pool suffers net photoinhibition (Aro et al., 2005; Nishiyama et al., 2005, 2006; Murata et al., 2007), leading to a decrease in photosynthetic capacity and potentially to a decrease in growth. To limit photoinhibition, photosynthetic cells use physiological processes that dissipate excess light energy into heat, thereby preempting the generation of toxic reactive oxygen species (Baroli et al., 2004; Holt et al., 2004) that can inhibit metabolism, notably including the PSII repair processes (Nishiyama et al., 2006; Murata et al., 2007). These excitation dissipation mechanisms manifest as a drop in PSII fluorescence yield termed nonphotochemical quenching of fluorescence (NPQ). In land plants and characterized chlorophytes, NPQ is notably associated with changes in light-harvesting complex conformation along with pigmentation changes (Demmig-Adams and Adams, 1992; Baroli et al., 2004; Holt et al., 2004; Li et al., 2004).

The specialization of *Ostreococcus* ecotypes to contrasting environments suggests that they may have evolved distinct capacities to cope with rapid fluctuations in light. Here, we investigate this question by subjecting three different *Ostreococcus* ecotypes to short-term increases in light irradiance to uncover their capacities for PSII repair and susceptibilities to photoinactivation. We use a target theory approach (Nagy et al., 1995; Sinclair et al., 1996) to parameterize their susceptibility to primary photoinactivation in a form useful for predicting and modeling responses to changes in irradiance. We moreover compare the *Ostreococcus* strains to a much larger prasinophyte derived from temperate surface waters, *Pyramimonas obovata*, to explore how cell size can influence photophysiology in the prasinophytes.

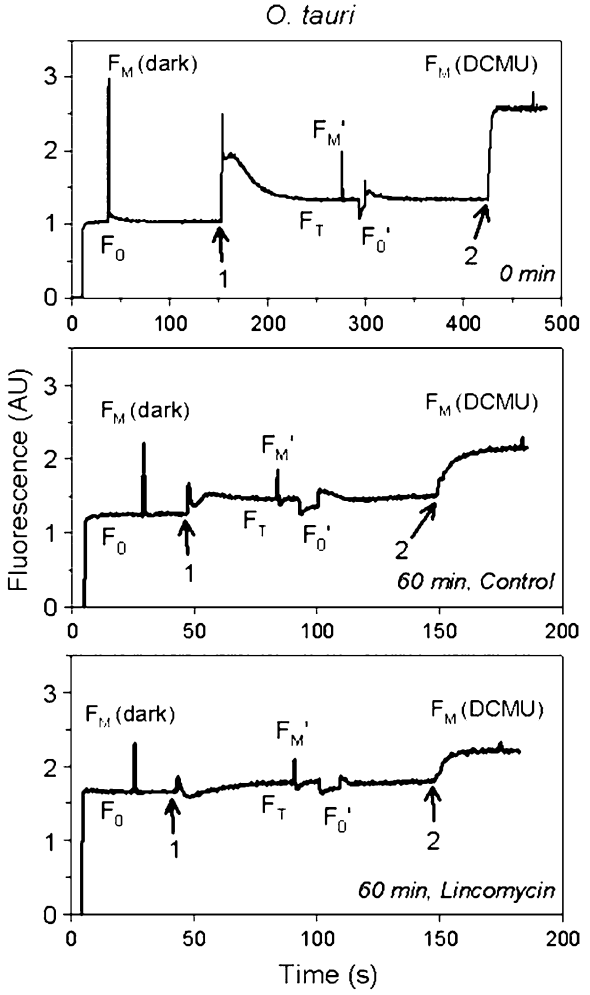

Figure 1. Examples of PAM fluorescence traces from *O. tauri* grown under low light, before the beginning of the experiment (top graph) and after 60 min of high-light exposure for control (middle graph) and lincomycin-treated (bottom graph) cells. F_0, Basal fluorescence recorded under modulated light only; F_M (dark), maximum fluorescence recorded in the dark upon triggering of a multiple-turnover saturating light pulse; F_T, fluorescence under actinic light; F_M', maximum fluorescence under actinic light; F_0', basal fluorescence under actinic light, recorded by turning off the actinic light for a short time; F_M (DCMU), maximum fluorescence under saturating light in the presence of DCMU. Arrow 1 indicates actinic light turned on, and arrow 2 indicates injection of DCMU. AU, Arbitrary units.

RESULTS

PSII Function during Irradiance Increase

For each sampling time point, we recorded a pulse amplitude modulation (PAM) fluorescence trace for the control and the lincomycin-treated cultures in order to measure different levels of fluorescence. Figure 1 depicts three typical examples of these traces for *O. tauri*, at the beginning of the experiment and after 60 min of high-light exposure, in the control culture and the lincomycin-treated culture. High-light exposure induced a progressive decrease in the maximal fluorescence levels and a slight increase of the basal fluorescence level. Lincomycin treatment additionally induced a more pronounced rise of the basal fluorescence level (F_0).

Inactivation of PSII reaction centers during high-light exposure in the four prasinophyte species was monitored using the PSII quantum yield (F_v/F_m; Fig. 2) in control and lincomycin-treated cultures. The portions of these curves corresponding to the high-light treatment were used to parameterize the PSII repair rate (R_{PSII}) and the effective target size for photoinactivation of PSII in the absence of repair (σ_i), estimated as the exponential decay in PSII function plotted versus cumulative incident photon dose per area, for each strain (Table I; for further details regarding this approach, see "Materials and Methods" and Six et al., 2007).

All four strains showed some net photoinhibition of PSII function, even in the subcultures with ongoing PSII repair (Fig. 2). This inhibition was most severe in the deepwater *O.* sp. RCC809 and least severe in *P.*

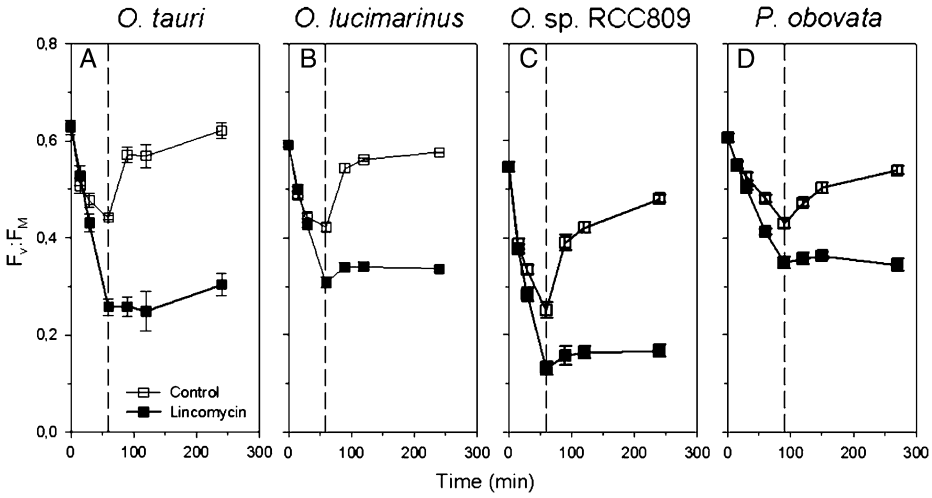

Figure 2. Changes in PSII quantum yield (F_v/F_m) in the four prasinophytes during 60 to 90 min of exposure to high light, followed by a 3-h recovery period. White symbols represent control culture, and black symbols represent lincomycin-treated culture ($n = 4 \pm$ SE). The dashed line delineates the high-light treatment and recovery periods.

obovata. The cultures treated with lincomycin to block PSII repair (Fig. 2, black symbols) showed that *O.* sp. RCC809 suffered a high primary susceptibility to photoinactivation, since PSII function dropped sharply when PSII repair was blocked. In marked contrast, the large-celled *P. obovata* showed less primary susceptibility to photoinactivation when PSII repair was blocked, so even a modest PSII repair rate was sufficient to largely counter the effects of the high-light treatment. *O. tauri* showed strong PSII repair, which partially countered the primary photoinactivation observed when PSII repair was blocked (Fig. 2, black symbols). Furthermore, *O. tauri* and *Ostreococcus lucimarinus* showed full recovery of PSII function during the low-light recovery period, whereas *O.* sp. RCC809 and *P. obovata* did not.

The slight increase in F_v/F_m observed after the lincomycin-treated cells were shifted back to their initial light condition was likely due to relaxation of a slow kinetic phase of NPQ, termed NPQs (see below).

D1 Protein Variations

Changes in D1 protein content were followed by immunoquantitation. During the high-light challenge, all of the prasinophytes were able to maintain or even increase their pool of D1 protein when their repair cycle was active (Fig. 3), demonstrating active synthesis of D1 protein. In the *Ostreococcus* cultures blocked by lincomycin, D1 content dropped sharply during high-light exposure. This drop was slightly more pronounced in *O. tauri* and *O. lucimarinus* than in *O.* sp. RCC809. In *P. obovata*, the lincomycin-treated cells only showed a significant drop in D1 protein compared with the control cultures after 90 min of high-light treatment (Fig. 3). This is in agreement with the low repair rates detected in this species (Table I). The retention of D1 protein in lincomycin-treated *P. obovata*, even though PSII activity was dropping (Fig. 2D), shows that, in this species, clearance of D1 protein lags behind the photoinactivation process. Similarly, in lincomycin-treated *O.* sp. RCC809, the clearance of D1 protein lags somewhat behind the decline in PSII activity (Fig. 2C), whereas in *O. tauri* and *O. lucimarinus*, the decline in PSII activity was approximately parallel to the decline in D1 content.

PSII Effective Absorption Cross Sections

When grown under low irradiance, the four prasinophytes exhibited distinct effective absorption cross sections for PSII (σ_{PSII}; Fig. 4), estimated from PSII fluorescence rise kinetics. Among the *Ostreococcus* spp., the deepwater strain RCC809 showed the largest σ_{PSII}, in agreement with its ecological niche (105 m depth; Rodríguez et al., 2005; Six et al., 2008) where light irradiance is low (Partensky et al., 1996). *O. tauri* and *P. obovata* showed an apparently small σ_{PSII}.

PSII effective absorption cross sections increased in *O. tauri* and *O. lucimarinus* in response to high light. This increase reflects antenna connectivity: as PSII

Table I. *Origin, cell size, Chl b:a, R_{PSII}, and σ_i for Ostreococcus spp. and P. obovata (n = 4, ± SE)*

Parameter	*O. tauri*	*O. lucimarinus*	*O.* sp. RCC809	*P. obovata*
Origin	Thau Lagoon, surface	California Current, surface	Tropical Atlantic Ocean, 105 m	Sargasso Sea, surface
Cell diameter (μm)	1–2	2	1–2	6–8
Chl *b:a*	0.55 ± 0.04	0.43 ± 0.1	0.8 ± 0.13	0.68 ± 0.09
R_{PSII} (PSII s^{-1})	$1.4 \times 10^{-4} \pm 1.7 \times 10^{-5}$	$0.8 \times 10^{-4} \pm 0.4 \times 10^{-5}$	$1.5 \times 10^{-4} \pm 1.0 \times 10^{-5}$	$0.5 \times 10^{-4} \pm 0.3 \times 10^{-5}$
σ_i (Å^2)	$-1.2 \times 10^{-4} \pm 7 \times 10^{-6}$	$-0.9 \times 10^{-4} \pm 3 \times 10^{-6}$	$-1.8 \times 10^{-4} \pm 11 \times 10^{-6}$	$-0.5 \times 10^{-4} \pm 2 \times 10^{-6}$

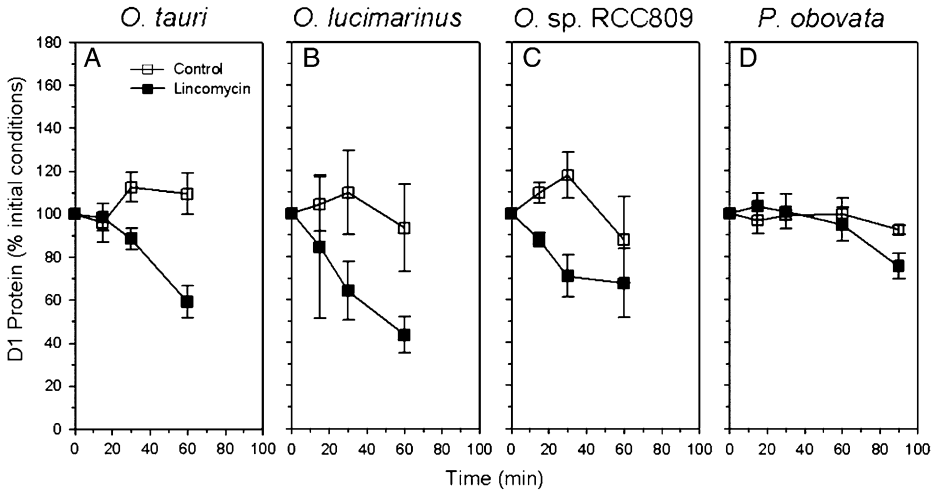

Figure 3. Changes in D1 protein content in the four prasinophytes during 60 to 90 min of exposure to high light. White symbols represent control culture, and black symbols represent lincomycin-treated culture ($n = 4 \pm$ SE).

reaction centers close or become photoinactivated, the antenna complex may serve adjacent antennae connected to open functional PSII centers, causing a dynamically increasing effective antenna size as reaction centers close (Hecks et al., 1996; Stirbet et al., 1998). After 3 h of recovery, σ_{PSII} decreased back toward values close to the initial conditions, at least in cells with active PSII repair cycles (white symbols). *O. tauri* appeared to develop the highest antenna connectivity, with σ_{PSII} doubling within 60 min of high-light challenge in the presence of lincomycin (Fig. 4A). In our experimental conditions, the deepwater strain *O.* sp. RCC809 (Fig. 4C) and *P. obovata* (Fig. 4D) showed little change in σ_{PSII} during the high-light treatment. They were also the strains that showed evidence for retention of pools of photoinactivated PSII (compare Fig. 2, C and D, with Fig. 3, C and D). In *O.* sp. RCC809, the Poisson model fits of the fluorescence rise kinetics were less robust in the strongly photoinhibited culture aliquots and for the 60-min time point in the presence of lincomycin, for which we were unable to obtain good quality fits.

Changes in Pigmentation

Modifications of cell pigmentation during high-light exposure were monitored using HPLC. Among the numerous pigments typically present in *Ostreococcus* cells, chlorophyll (Chl) *a*, Chl *b*, magnesium divinyl phaeoporphyrin a_5, uriolide, neoxanthin, prasinoxanthin, micromonal, and dihydrolutein showed steady levels throughout the high-light shift and the subsequent recovery period. The chromatograms from *P. obovata* showed no variations for Chl *a*, Chl *b*, magnesium divinyl phaeoporphyrin a_5, neoxanthin, and three of the four unknown carotenoids. Chl *b*:*a* levels ranged from 0.8 in the deepwater *O.* sp. RCC809 down to 0.4 in the surface *O. lucimarinus*. This range of values is comparable with pigment analyses performed on other prasinophytes (Rodriguez et al., 2006).

Figure 5 shows the deepoxidation state (DES) of the photoprotective xanthophyll cycle (involving violaxanthin, antheraxanthin, and zeaxanthin) during the high-light challenge. In the four prasinophytes, xanthophyll cycle (Demmig-Adams and Adams, 1992; Baroli et al., 2004; Holt et al., 2004) was induced in

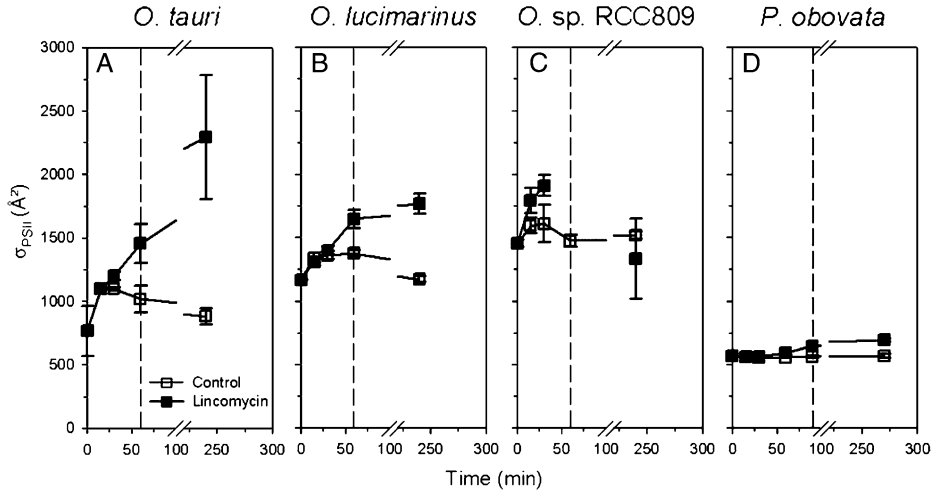

Figure 4. Changes in PSII effective absorption cross section, estimated from flash fluorescence rise kinetics, in the four prasinophytes during 60 to 90 min of exposure to high light followed by a 3-h recovery period. White symbols represent control culture, and black symbols represent lincomycin-treated culture ($n = 4 \pm$ SE). The dashed line delineates the high-light treatment and recovery periods.

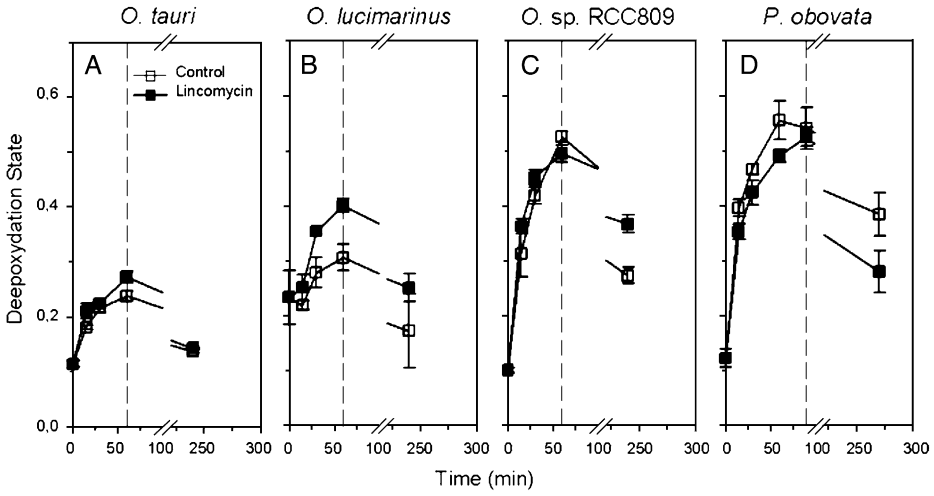

Figure 5. Changes in deepoxidation state of the xanthophyll cycle in the four prasinophytes during 60 to 90 min of exposure to high light followed by a 3-h recovery period. White symbols represent control culture, and black symbols represent lincomycin-treated culture ($n = 4 \pm$ SE). The dashed line delineates the high-light treatment and recovery periods.

response to high light and then relaxed during the recovery period. The amplitude of deepoxidation was different among the four species. *O. tauri* and *O. lucimarinus* showed moderate xanthophyll cycle induction (Fig. 5, A and B). *O.* sp. RCC809 and *P. obovata* developed a high xanthophyll deepoxidation in response to high light, reaching almost twice the DES value of *O. tauri* after 60 min of light stress. Furthermore, there was no evidence of a dependence on concurrent chloroplastic protein synthesis for DES buildup in these species, as control and lincomycin-treated cells showed similar patterns.

In addition to the deepoxidation activity, the three *Ostreococcus* strains increased their pool size of the three xanthophylls involved in the xanthophyll cycle (Fig. 6) in response to high-light exposure. The xanthophyll pool size reached after 60 min was maintained after the 3-h recovery period. Among these three strains, the deepwater *O.* sp. RCC809 displayed the lowest xanthophyll-to-Chl *a* ratio. *P. obovata* showed a different pattern with nearly steady xanthophyll pool size for the control cultures and a decreasing one in the presence of lincomycin in response to irradiance increase. This was followed by a sharp increase of the xanthophyll pool size after 60 min of high-light exposure and through the 3-h recovery period.

Concomitantly, after a slight initial drop, lutein levels increased moderately in *O. lucimarinus* and strongly in the deepwater strain *O.* sp. RCC809. In contrast, *O. tauri* showed only trace levels of lutein after 60 min of high-light exposure (Fig. 7). Lutein accumulation was not dependent on chloroplastic protein synthesis, as control and lincomycin-treated cells showed similar patterns. In the larger prasinophyte *P. obovata*, similar to the xanthophyll pool size, lutein dropped and then reaccumulated after about 60 min of high-light exposure and during the recovery period (Fig. 7D), as if the response was delayed.

Among the four prasinophytes, the carotene content (β,β-carotene and β,ε-carotene) was affected by the treatment only in the deepwater strain *O.* sp. RCC809,

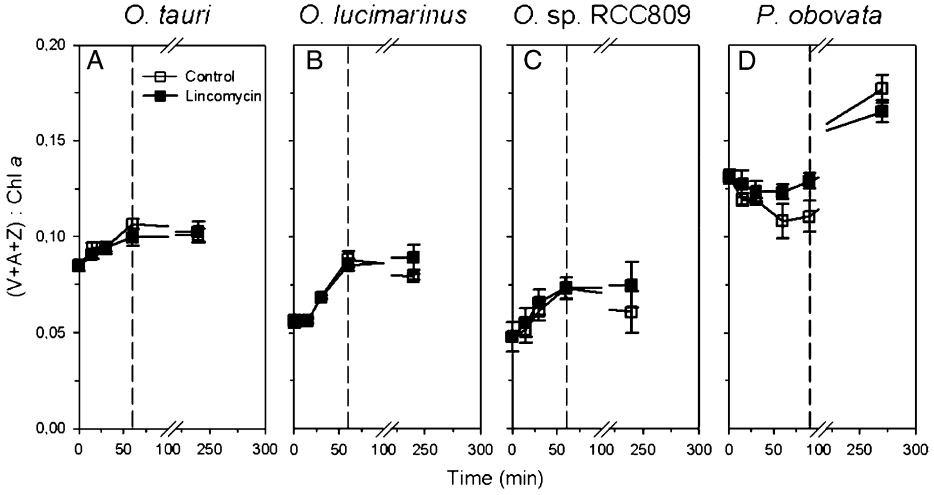

Figure 6. Changes in the sum of violaxanthin, antheraxanthin, and zeaxanthin-to-Chl *a* ratio in the four prasinophytes during 60 to 90 min of exposure to high light followed by a 3-h recovery period. White symbols represent control culture, and black symbols represent lincomycin-treated culture ($n = 4 \pm$ SE). The dashed line delineates the high-light treatment and recovery periods.

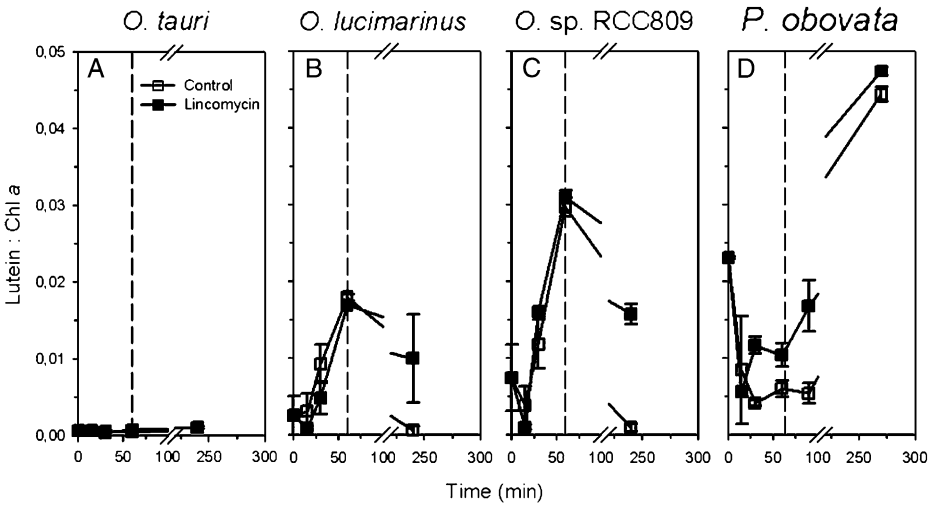

Figure 7. Changes in lutein-to-Chl *a* ratio in the four prasinophytes during 60 to 90 min of exposure to high light followed by a 3-h recovery period. White symbols represent control culture, and black symbols represent lincomycin-treated culture ($n = 4 \pm$ SE). The dashed line delineates the high-light treatment and recovery periods.

decreasing by 3-fold (Fig. 8). Control and lincomycin-treated cells did not show any difference in carotene dynamics, indicating no dependence on concurrent chloroplastic protein synthesis. In *Pyramimonas*, a carotenoid eluting at 17 min (spectrum maximum absorption of 417, 444, and 472 nm) was down-regulated by 50% in response to high light, and its content was fully recovered after the 3-h low-light period (data not shown). We were unfortunately unable to identify this pigment.

NPQ Induction

In the four prasinophyte strains, analyses of the fluorescence induction traces revealed two main kinetic components of NPQ. In these cells grown under 30 μmol photons m^{-2} s^{-1}, dynamic NPQ (NPQd) was induced and relaxed within 1 to 3 min and largely relaxed upon addition of 3-(3,4-dichlorophenyl)-1,1-dimethylurea (DCMU) to block electron transport. NPQd did not correlate with measured DES to any extent. NPQd was low, ranging from about 0.2 (*P. obovata*) to 0.4 (*O. tauri* and *O. lucimarinus*; Fig. 9), and increased during the low-light recovery period. This increase during recovery was blocked in the cells treated with lincomycin, suggesting that the magnitude of NPQd was related to the content of active PSII centers. In addition to NPQd, the prasinophytes showed a slower kinetic phase of NPQ, which we estimated as sustained NPQs = $(F_m^0 - F_m)/F_m$ (see "Materials and Methods"). Sustained NPQs compares the initial F_m at the beginning of the experiment, measured in the low-light cells and dark adapted for 5 min before any high-light treatment, with F_m measured after 5 min of dark adaptation at each time point during the course of the high-light treatment and subsequent low-light recovery. Sustained NPQs started at 0 (by definition) and rose during the high-light treatment to 0.2 (*O. lucimarinus*) and to 0.7 (*O.* sp. RCC809) over 60 min (Fig. 10). It then relaxed during the subsequent low-light recovery with similar kinetics. Sustained NPQs was generally not affected by the

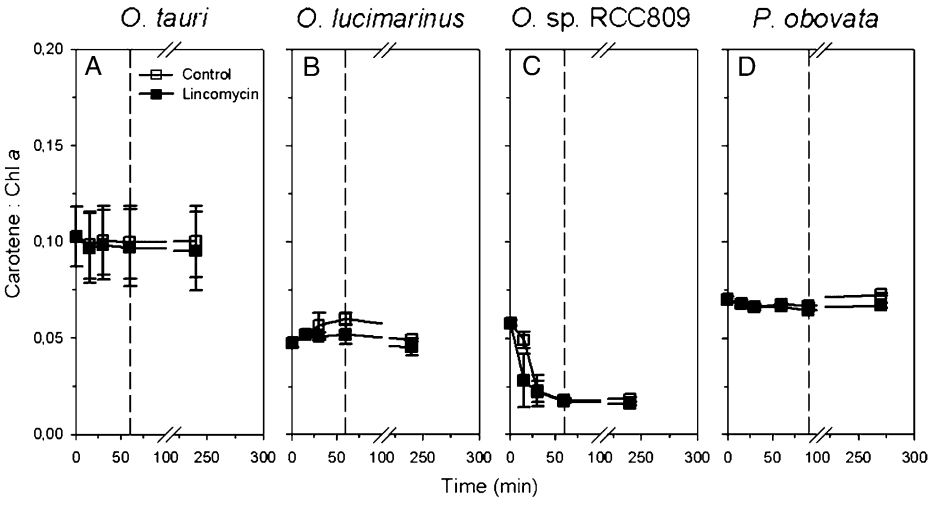

Figure 8. Changes in carotene (β,β-carotene and β,ε-carotene)-to-Chl *a* ratio in the four prasinophytes during 60 to 90 min of exposure to high light followed by a 3-h recovery period. White symbols represent control culture, and black symbols represent lincomycin-treated culture ($n = 4 \pm$ SE). The dashed line delineates the high-light treatment and recovery periods.

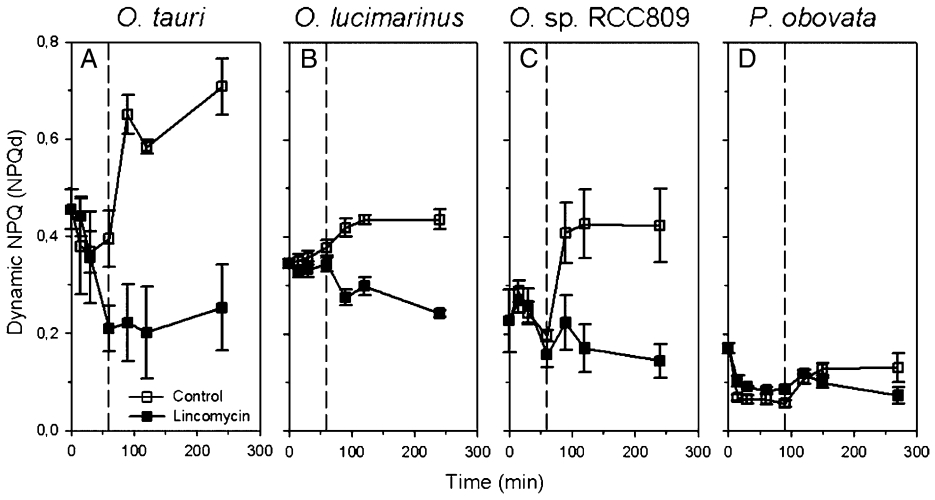

Figure 9. Changes in NPQd in the four prasinophytes during 60 to 90 min of exposure to high light followed by a 3-h recovery period. White symbols represent control culture, and black symbols represent lincomycin-treated culture ($n = 4 \pm$ SE). The dashed line delineates the high-light treatment and recovery periods.

presence of lincomycin and so did not seem to rely on concurrent chloroplastic protein synthesis. Moreover, it correlated well with the measured DES (Fig. 11).

DISCUSSION

Light Capture in *Ostreococcus* Ecotypes

The general photophysiology of *Ostreococcus* ecotypes differs considerably depending on their ecological niche (Rodríguez et al., 2005; Cardol et al., 2008; Six et al., 2008). Among the *Ostreococcus* strains investigated here, the two surface ecotypes showed moderate PSII effective absorption cross sections while the deepwater *O.* sp. RCC809 had the largest PSII effective absorption cross section, in agreement with previous work (Rodríguez et al., 2005; Cardol et al., 2008; Six et al., 2008) and its origin (105 m depth) where irradiance is low (Partensky et al., 1996). Likewise, *O.* sp. RCC809 displayed higher ratios of accessory pigments to Chl *a* (data not shown; Rodríguez et al., 2005, 2006; Six et al., 2005, 2008), except for the xanthophyll cycle pigments. Interestingly, in the face of PSII photoinhibition, the surface *O. tauri* and *O. lucimarinus* manifested PSII antenna connectivity, with increasing effective absorbance cross sections for the remaining PSII. This mechanism represents a means to maintain photosynthesis under light stress and thus appears useful to organisms that must cope with large irradiance fluctuations. Although the presence of a large functional antenna in *O.* sp. RCC809 might suggest that antenna connectivity could easily occur, this strain inhabiting the bottom of the euphotic zone did not manifest antenna connectivity in the face of PSII photoinhibition, at least in our experimental conditions.

PSII Photoinactivation and Repair in *Ostreococcus* Ecotypes

We investigated the responses of four prasinophytes to the challenge of a 10× increase in irradiance under conditions that provoked reversible photoinhibition.

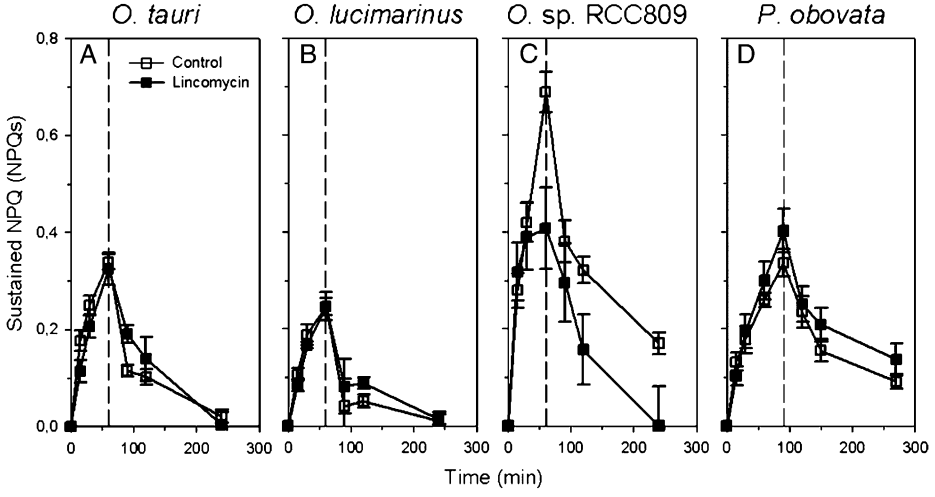

Figure 10. Changes in sustained NPQs in the four prasinophytes during 60 to 90 min of exposure to high light followed by a 3-h recovery period. White symbols represent control culture, and black symbols represent lincomycin-treated culture ($n = 4 \pm$ SE). The dashed line delineates the high-light treatment and recovery periods.

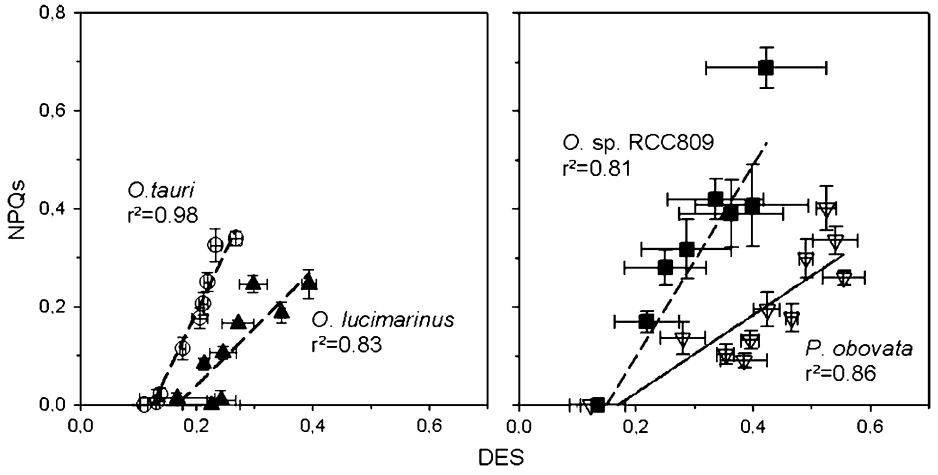

Figure 11. Correlation between sustained NPQs and xanthophyll DES in the four prasinophytes during 60 to 90 min of exposure to high light followed by a 3-h recovery period. White circles represent *O. tauri,* black triangles represent *O. lucimarinus,* black squares represent *O.* sp. RCC809, and white triangles represent *P. obovata* ($n = 4 \pm$ SE).

Six et al. (2007) exposed a panel of marine picocyanobacteria to a similar moderate increase in light and found that a direct photoinactivation target size model (Nagy et al., 1995; Sinclair et al., 1996), with the decrease in PSII quantum yield plotted versus cumulative incident photon dose per area, gave consistent fits across species, as opposed to a more complex model of photoinactivation as a side effect of photons captured via the PSII antenna. The σ_i parameterization is consistent with most photoinactivation being provoked by a direct hit upon the manganese cluster of PSII, which knocks out water splitting and then leads to photooxidative destruction of the reaction center (Hakala et al., 2005; Sarvikas et al., 2006; Tyystjarvi, 2008). This mechanism is most prevalent under UV and blue light, which are best absorbed by the manganese cluster (Sarvikas et al., 2006). The different *Ostreococcus* ecotypes are now interesting models for studying PSII photoinactivation in chlorophytes because they have simple and similar cellular optics and similar pigmentation but show different PSII effective absorption cross sections, even when grown under a common light level.

O. sp. RCC809 showed the highest primary susceptibility to photoinactivation, parameterized as $\sigma_i = -1.8 \times 10^{-4}$ Å^2, that has as yet been measured among phytoplankton grown under comparable low-light conditions, including other prasinophytes (this study), the freshwater cyanobacterium *Synechocystis* sp. PCC 6803 (Nagy et al., 1995), three strains of marine *Synechococcus*, two strains of *Prochlorococcus* (Six et al., 2007), one strain of *Pelagococcus*, *Porphyridium cruentum* (D.A. Campbell, unpublished data), and 10 species of marine diatoms to date (Z.V. Finkel, unpublished data). The three *Ostreococcus* strains all relied on active PSII repair to partially counter photoinactivation, but *O.* sp. RCC809 showed incomplete recovery from the more severe photoinhibition it sustained.

PSII repair involves the clearance of photoinactivated D1 proteins through an active process that, in species analyzed to date, is mediated primarily by the FtsH protease system (Silva et al., 2003), with parallel reassembly of PSII subcomplexes with a newly synthesized D1 protein (Aro et al., 1993; Murata et al., 2007). All four species of prasinophytes were able to maintain their total pools of D1 protein during the 10× high-light challenge treatment. Nevertheless, the D1 immunoquantitation includes both D1 from functional PSII and D1 proteins, which, although still covalently intact, are derived from photoinactivated PSII centers. In all four species, the F_v/F_m measure of PSII function dropped significantly even in the control subcultures, which maintained PSII repair and D1 protein content, although the latter data showed some scatter among replicates. This suggests that under the 10× high-light challenge, a likely rate-limiting step in the overall PSII repair cycle was the removal of D1 from photoinactivated PSII centers, since D1 level was maintained while PSII quantum yield was declining. When PSII repair was blocked by addition of the lincomycin inhibitor, PSII quantum yield and D1 protein content declined in parallel in *O. lucimarinus*, thereby showing good clearance of photoinactivated D1. In the other species, and particularly in *O.* sp. RCC809 and *P. obovata*, the decline in D1 lagged behind the decline of the PSII quantum yield. Thus, in *O.* sp. RCC809 and *P. obovata*, clearance of photoinactivated D1 is likely a rate-limiting step on the PSII repair cycle under a high-light challenge.

Pigment Dynamics and Excitation Dissipation

Carotene levels were stable in *O. tauri* and *O. lucimarinus* but showed a sharp 72% decline in *O.* sp. RCC809. In oxygenic photosynthetic complexes, carotenes are thought to be located on the D2 protein of PSII (only two carotene molecules per complex) and on the PsaAB proteins of the PSI complex (a larger number of molecules per complex), acting as quenchers of singlet oxygen (Telfer, 2005). Given the extent of the drop observed in *O.* sp. RCC809, carotene from both photosystems was lost during high-light exposure. It should be noted that *Ostreococcus* strains contain both α- and β-carotenes, but, to our knowledge, their dif-

ferential roles and locations are as yet unknown. The clear distinction in carotene dynamics in *O.* sp. RCC809 compared with the other strains indicates a pronounced oxidative stress situation (Krieger-Liszkay, 2005; Telfer, 2005; Krieger-Liszkay et al., 2008) during the high-light challenge compared with the other strains. This indicator of reactive oxygen species (ROS) toxicity is consistent with the large PSII antenna in *O.* sp. RCC809, which could potentiate ROS production under excess light. In leaves, Sarvikas et al. (2006) found about 25% variation in primary susceptibility to photoinactivation related to the induction of NPQ. Since the direct hit model for PSII photoinactivation, parameterized by σ_i, does not relate directly to photosynthetic antenna size or to ROS, a fraction of photoinactivation in leaves relates to other processes such as ROS toxicity. In parallel, one may suspect that the apparent high susceptibility to photoinactivation in *O.* sp. RCC809 reflects supplemental photoinactivation pathways, beyond the direct hit model. Furthermore, ROS toxicity in *O.* sp. RCC809 is consistent with the findings of Cardol et al. (2008), who showed an alternative electron transport flux in this strain, with electrons dumped from PSII back to oxygen via the plastid terminal oxidase (Josse et al., 2000) as a means to dissipate excess reductant while driving accumulation of a transthylakoidal pH gradient. Such a mechanism would, a priori, carry a high risk for ROS formation, notably in the vicinity of carotenes.

The four prasinophytes show the full complement of chlorophyte xanthophyll cycle pigments, zeaxanthin, antheraxanthin, and violaxanthin, which are involved in mediating a major transthylakoidal pH-dependent mechanism for light energy dissipation (Baroli et al., 2004; Holt et al., 2004). The 10× light challenge treatment provoked significant increases in the xanthophyll deepoxidation state, especially in *O.* sp. RCC809 and *P. obovata*, with subsequent relaxation during the recovery period. The changes in deepoxidation ratio were nearly parallel in subcultures without or with lincomycin, so these changes in deepoxidation ratio do not require concurrent chloroplastic protein synthesis, and indeed the violaxanthin deepoxidase genes are nucleus encoded. Among the *Ostreococcus* strains, xanthophyll cycle activity was high in *O.* sp. RCC809, showing that this strain was quite stressed by the high-light challenge. *O.* sp. RCC809 showed the lowest initial xanthophyll-to-Chl *a* ratio, whereas the lagoon strain *O. tauri* showed a value almost 2-fold higher, a feature that probably allows this strain to easily cope with large and sudden irradiance increases.

In land plants, the amplitude and/or kinetics of NPQ can often be correlated with the light-dependent deepoxidation of violaxanthin and pool size of the xanthophylls involved in the xanthophyll cycle (Johnson et al., 2008). Prasinophytes, however, show different NPQ and xanthophyll cycle properties. For example, the prasinophyte *Mantoniella squamata* can be distinguished from other photosynthetic organisms by a xanthophyll cycle that undergoes a single deepoxidation step under excess light, leading to the accumulation of monoepoxide xanthophyll antheraxanthin (Gilmore and Yamamoto, 2001). In this study, the slow kinetics of induction and relaxation make the sustained NPQs superficially look like the "q_I" category of NPQ related to photoinhibition. But the induction and relaxation of sustained NPQs is not affected by chloroplastic protein synthesis, and sustained NPQs is rather correlated with DES. This sustained NPQ can thus be considered as a slow induction/slow relaxation phase of quenching of total PSII fluorescence mediated by the xanthophyll cycle and possibly interacting with the accumulation of lutein (Ruban et al., 2007).

Lutein accumulation varied across the *Ostreococcus* strains. A conversion from lutein epoxide to lutein has been reported in various chlorophytes, particularly in shade-adapted species exposed to strong light (Matsubara et al., 2005, 2007; Forster et al., 2009). We did not find a specific and exclusive correlation between lutein accumulation and other photoprotection parameters, although the lutein accumulation did track the induction and relaxation of NPQs in *O. lucimarinus* and in *O.* sp. RCC 809. Lutein accumulation was slower than the accumulation and deepoxidation of the other photoprotective xanthophylls and thus seems to be involved in a longer term photoprotective mechanism (Matsubara et al., 2005, 2007; Forster et al., 2009). Interestingly, lutein accumulation was not dependent on concurrent chloroplastic protein synthesis, and there was no apparent conversion from the likely precursor dihydrolutein. *O.* sp. RCC809 showed a higher accumulation than the surface strain *O. lucimarinus*, while *O. tauri* contained very little lutein after 60 min of high-light exposure. This is in agreement with the deepwater *O.* sp. RCC809 being more sensitive to high-light treatment than the surface strains. This capacity of a low-light-adapted prasinophyte to induce lutein accumulation demonstrates that this response is conserved across a wide range of the chlorophytes but manifests primarily in those species adapted to low light (Matsubara et al., 2005, 2007; Forster et al., 2009).

Comparison of the Picoplanktonic *Ostreococcus* with the Larger *P. obovata*

The prasinophyte *P. obovata* has an approximately 500-fold larger biovolume than the picoplanktonic *Ostreococcus* strains. Biovolume has strong influences on light capture because of pigment packaging effects, which lower the efficacy of light capture per pigment in larger cells (Kirk, 1976; Morel and Bricaud, 1981; Agusti, 1991; Finkel, 2001). *P. obovata* showed the lowest PSII effective absorption cross section value but an intermediate Chl *b*:*a* of 0.7. This suggests that the smaller σ_{PSII} in *P. obovata* compared with *Ostrecoccus* spp. is likely a result of pigment self-shading effects rather than a decrease in antenna complexes per reaction center, monitored through Chl *b*:*a*. *P.*

obovata, moreover, suffered less primary photoinactivation under the increased light compared with the *Ostreococcus* strains. This relatively low σ_i may also be a consequence of the larger pigment self-shading effect in *P. obovata* compared with the picoprasinophyte *Ostreococcus*. The slow R_{PSII} in *P. obovata* is thus adequate, given the low susceptibility to primary photoinactivation. Expressed differently, under conditions of moderately high-light stress, the small *O. tauri* could replace a PSII within about 1 h and 20 min, while *P. obovata* required about 4 h and 40 min to replace a PSII; in parallel, *P. obovata* also experienced slower photoinactivation. Compared with *Ostreococcus* strains, *P. obovata* showed a large xanthophyll pool and high violaxanthin deepoxidation despite the low repair activity, suggesting that it relies more on static screening and on dissipation of excess light energy rather than on repair activity to protect the PSII centers.

P. obovata showed a different pattern of lutein variations, with loss of lutein during high-light exposure, followed by lutein accumulation during the low-light recovery period. Similar lutein degradation has recently been reported in avocado (*Persea americana*) plants (Forster et al., 2009). Metabolic processes scale with organism size (Finkel, 2001; Gillooly et al., 2001), so that on a per volume or per biomass basis, small cells have generally higher metabolic rates. It is possible that the lutein synthesis was delayed in *P. obovata* compared with the metabolically faster *Ostreococcus* strains.

CONCLUSION

While *Ostreococcus* ecotypes are all able to induce PSII repair to counter increased light, they differ in their effective target size for primary photoinactivation (σ_i). The large antenna of deepwater strains is likely a major site of ROS formation, which could enhance alternative paths of PSII photoinactivation during high-light exposure. Comparison with the response of a much larger prasinophyte suggests that cell size has a significant influence on the regulation of light use in prasinophytes. Self-shading in larger cells decreases absorbed light per pigment but also slows PSII photoinactivation rates. During evolution, the photophysiology of *Ostreococcus* spp. has been adjusted to their minute size, which implies a negligible package effect and relatively high PSII repair rates to counter their large effective target sizes for photoinactivation.

MATERIALS AND METHODS

Culture Conditions and High-Light Treatments

Cultures of *Ostreococcus tauri* (strain OTH95, isolated from Thau Lagoon, France), *Ostreococcus lucimarinus* (strain CCMP2514, isolated from the California Current), *Ostreococcus* sp. RCC809 (isolated from 105 m in the tropical Atlantic Ocean), and *Pyramimonas obovata* (strain CCMP722, isolated from near surface water of the Sargasso Sea) were grown in polystyrene flasks (Corning) containing K medium (Keller et al., 1987) at 21°C ± 1°C under 30 μmol photons m^{-2} s^{-1} continuous white light provided by fluorescent tubes (daylight; Sylvania) and measured in the culture flasks using a microspherical quantum sensor (US-SQS; Walz) connected to a Li-Cor quantameter (LI-250; Li-Cor). The *O. tauri* strain was obtained from the Roscoff Culture Collection (strain RCC745), and the other prasinophytes were from the Centre for Culture of Marine Phytoplankton.

Cultures from the exponential growth phase were split into two flasks, with 500 μg mL^{-1} lincomycin added to one flask in order to block chloroplast protein synthesis (Bachmann et al., 2004), thereby inhibiting PSII repair (Tyystjarvi and Aro, 1996). Both flasks were incubated in the dark for 10 min to allow the lincomycin to exert its effect and then placed at 21°C under blue light irradiance of 300 μmol photons m^{-2} s^{-1} adjusted with colored filters (LEE filter no. 183; Panavision) for 60 min (*Ostreococcus* strains) or 90 min (*P. obovata*). Blue treatment light was chosen to partially mimic an average marine light field and to provide efficient PSII photoinactivation (Sarvikas et al., 2006). Samples were collected repeatedly for Chl fluorescence analyses and for filtration onto glass fiber filters, which were flash frozen for later immunoblotting and pigment analyses. Following the high-light treatment, the remaining cultures were returned to their initial growth light of 30 μmol photons m^{-2} s^{-1} for a 3-h recovery period.

PAM Fluorescence Measurements

Chl fluorescence yield data were collected using a Xe-PAM fluorometer (Walz) connected to a temperature-controlled cuvette holder (Walz). At each sampling point, an aliquot of culture was dark adapted for 5 min to relax photosynthetic activity. A modulated beam (4 Hz) was used to measure F_0, followed by a saturating white-light pulse (4,000 μmol photons m^{-2} s^{-1}) to measure F_m (dark). Actinic light was then administered with identical conditions to the treatment light (300 μmol blue photons m^{-2} s^{-1}), and F_t, the steady fluorescence level in a light-acclimated sample, was measured. Another saturating pulse was then applied to measure maximal fluorescence in the light (F_m'). Actinic light was then turned off for a few seconds in order to record the basal level of fluorescence in the light-acclimated sample (F_0'). Finally, 1 mM of the PSII inhibitor DCMU was added, and once a steady state was achieved, a final light pulse was triggered to determine the F_m (DCMU) with linear electron transport blocked. Figure 1 shows typical fluorescence traces with the corresponding fluorescence levels. The maximum quantum yield of PSII photochemistry was then estimated as:

$$F_v/F_m = (F_m - F_0)/F_m$$

Two different kinetic components of NPQ were estimated. The dynamic, short-term NPQ (Vankooten and Snel, 1990) induced during the fluorescence measurement was estimated as:

$$\mathrm{NPQd} = (F_m - F_m')/F_m'$$

This parameter is the typical NPQ estimate that compares F_m measured after dark acclimation with the F_m' measured under a treatment light. Upon exposure to the treatment light of 300 μmol photons m^{-2} s^{-1}, steady-state fluorescence stabilized within 2 min and F_m' was then measured. Subsequent addition of DCMU to the culture samples led to rapid and nearly complete reversal of NPQd within 1 min. NPQd, therefore, measures NPQ that is induced and reverses rapidly.

A second, slower kinetic component of NPQ was estimated as:

$$\mathrm{NPQs} = (F_m^0 - F_m)/F_m$$

F_m^0 was measured in cells taken from their initial low-light growth condition of 30 μmol photons m^{-2} s^{-1} and dark acclimated for 5 min. NPQs thus compares this F_m^0 with the F_m values measured at each time point during the high-light treatment and subsequent recovery periods. NPQs, therefore, measures NPQ that is sustained through the brief 5-min dark acclimation that precedes each fluorescence measurement. This comparison across the duration of the treatment period is valid because there was negligible change in Chl in the cultures (see "Results"), the treatments were short, and comparable optics were maintained across measurements. NPQs is not reversed by short-term

addition of DCMU, but it does slowly relax in cells returned to low light, even in the presence of lincomycin, which inhibits chloroplastic protein synthesis.

Photoinactivation Parameterization

F_v/F_m was plotted over time for both the control and lincomycin-treated subcultures, and exponential decay curves were fitted over the high-light treatment period. The R_{PSII} was estimated as the difference between the exponential decay rates in the absence and presence of lincomycin (Six et al., 2007). For the estimation of R_{PSII} and σ_i (see below), any initial decline in F_v/F_m during the first 15 min of high-light challenge was corrected by the magnitude of any subsequent increase in F_v/F_m in the culture fraction treated with lincomycin during the low-light recovery to separate photoinactivation from any influence of NPQs that was sustained during the dark acclimation period before measurement of F_v/F_m. These corrections were small and had little influence on the estimated R_{PSII} and σ_i parameters.

The effective target size for primary PSII photoinactivation (Nagy et al., 1995; Sinclair et al., 1996; Six et al., 2007) for blue light, termed σ_i (i standing for inactivation) and expressed in $Å^2$ $PSII^{-1}$, was estimated as the exponential decay for F_v/F_m in the absence of PSII repair plotted versus cumulative incident photon dose. The σ_i parameter does not represent the physical size of a target molecule or atom. Instead, using a Poisson target formulation, in units of area, it folds together the probability of absorbance of the photon with the probability that the absorbance event provokes the measured response, a drop in F_v/F_m. This formulation is a useful general parameterization for modeling photophysiology and is mechanistically consistent with the photoinactivation results and models of Hakala et al. (2005), Nishiyama et al. (2006), Sarvikas et al. (2006), and Six et al. (2007).

Fluorescence Induction Measurements

To determine the effective absorbance cross section for PSII photochemistry (Falkowski and Raven, 1997) under blue light σ_{PSII}, a culture aliquot was placed into a Satlantic FIRe fluorometer (Satlantic) and dark-adapted for 5 min, after which a 100-μs single-turnover flash was triggered by a blue light-emitting diode source (455 ± 20 nm), driving fluorescence to the maximal yield F_m for a single turnover flash. The fluorescence rise was analyzed using the FIREWORX script (A. Barnett, https://sourceforge.net/projects/fireworx/) for MATLAB software (Mathworks), and σ_{PSII} was estimated in accordance with the instrument-specific flash irradiance calibration factor provided by Satlantic. For each fluorescence induction rise, FIREWORX reports the statistical 95% confidence interval for the estimated σ_{PSII}. For a few measurements on photoinhibited samples, the fluorescence rise amplitudes were small, resulting in weak fits with confidence interval widths exceeding 40% of the estimated σ_{PSII}; therefore, such replicates were excluded from subsequent analyses.

Immunoquantitation of D1 Proteins

At each sampling point, 20 mL of culture was suctioned onto a glass-fiber filter, flash frozen in liquid nitrogen, and kept at −80°C until analysis. Immunoquantitations were carried out as described previously (Six et al., 2007; Brown et al., 2008; Garczarek et al., 2008). Filtered cell samples were thawed in 300 μL of protein solubilization buffer, and the proteins were extracted through several rounds of flash freezing in liquid nitrogen and subsequent thawing by sonication. A volume containing 1 μg of total protein of each sample was loaded on an E-PAGE 8% gel (Invitrogen), along with recombinant D1 standard protein (Agrisera) at a range of known concentrations. Proteins were then transferred onto a polyvinylidene difluoride membrane for 15 min using a dry iBlot Gel Transfer device (Invitrogen). After membrane blocking, primary antibody against the C-terminal part of the D1 subunit (Agrisera) was applied, followed by a secondary antibody coupled with horseradish peroxidase. The membranes were revealed by chemiluminescence using ECL Advance reagent (Amersham, GE Healthcare). Recombinant protein standard curves were used to estimate the target protein contents for the samples.

Pigment Analyses

For phytoplankton pigment analyses, a 20-mL volume of culture was filtered through a 25-mm-diameter Whatman GF/F glass fiber filter. The filter was immediately flash frozen and stored at −80°C until analysis. Pigments were extracted from the filter in 95% methanol and sonicated on ice (Sonicator Ultrasonic Processor XL 2010). The extracts were cleared from any filter debris by centrifugation and filtration over a 0.22-μm polytetrafluoroethylene syringe filter. A 50-μL extract was then injected in a reverse-phase C8 Waters Symmetry column (150 × 4.6 mm, 3.5 μm). Gradient elution was controlled by a Thermo Separation P4000 pump with gradient solvents present in the HPLC method developed by Zapata et al. (2000). Pigments were detected using a FL 3000 fluorescence detector in series with a photodiode array (UV 6000 LP) detector. Pigments were identified and quantified according to their retention time, absorbance spectrum, and comparison with standards from DHI (http://c14.dhigroup.com).

ACKNOWLEDGMENTS

We thank L. McIntyre for skilled maintenance of stock cultures, Z. Finkel for stimulating discussions, and Carolyn Dubois and Avery McCarthy for assistance with data analyses. We thank two anonymous reviewers for insightful and constructive comments.

Received April 29, 2009; accepted July 5, 2009; published July 8, 2009.

LITERATURE CITED

Agusti S (1991) Allometric scaling of light absorption and scattering by phytoplankton cells. Can Bull Fish Aquat Sci **48:** 763–767

Aro EM, Suorsa M, Rokka A, Allahverdiyeva Y, Paakkarinen V, Saleem A, Battchikova N, Rintamaki E (2005) Dynamics of photosystem II: a proteomic approach to thylakoid protein complexes. J Exp Bot **56:** 347–356

Aro EM, Virgin I, Andersson B (1993) Photoinhibition of photosystem 2: inactivation, protein damage and turnover. Biochim Biophys Acta **1143:** 113–134

Bachmann KM, Ebbert V, Adams WW, Verhoeven AS, Logan BA, Demmig-Adams B (2004) Effects of lincomycin on PSII efficiency, non-photochemical quenching, D1 protein and xanthophyll cycle during photoinhibition and recovery. Funct Plant Biol **31:** 803–813

Baldauf SL (2003) The deep roots of eukaryotes. Science **300:** 1703–1706

Baroli I, Gutman BL, Ledford HK, Shin JW, Chin BL, Havaux M, Niyogi KK (2004) Photo-oxidative stress in a xanthophyll-deficient mutant of Chlamydomonas. J Biol Chem **279:** 6337–6344

Brown CM, MacKinnon JD, Cockshutt AM, Villareal TA, Campbell DA (2008) Flux capacities and acclimation costs in *Trichodesmium* from the Gulf of Mexico. Mar Biol **154:** 413–422

Cardol P, Bailleul B, Rappaport F, Derelle E, Beal D, Breyton C, Bailey S, Wollman FA, Grossman A, Moreau H, et al (2008) An original adaptation of photosynthesis in the marine green alga *Ostreococcus*. Proc Natl Acad Sci USA **105:** 7881–7886

Chrétiennot-Dinet MJ, Courties C, Vaquer A, Neveux J, Claustre H, Lautier J, Machado MC (1995) A new marine picoeucaryote: *Ostreococcus tauri gen et sp nov* (Chlorophyta, Prasinophyceae). Phycologia **34:** 285–292

Courties C, Vaquer A, Trousselier M, Lautier J, Chrétiennot-Dinet MJ, Neveux J, Machado C, Claustre H (1994) Smallest eukaryotic organism. Nature **370:** 255

Demmig-Adams B, Adams WW (1992) Photoprotection and other responses of plants to high light stress. Annu Rev Plant Physiol Plant Mol Biol **43:** 599–626

Derelle E, Ferraz C, Rombauts S, Rouze P, Worden AZ, Robbens S, Partensky F, Degroeve S, Echeynie S, Cooke R, et al (2006) Genome analysis of the smallest free-living eukaryote *Ostreococcus tauri* unveils many unique features. Proc Natl Acad Sci USA **103:** 11647–11652

Diez B, Pedros Alio C, Massana R (2001) Study of genetic diversity of eukaryotic picoplankton in different oceanic regions by small-subunit rRNA gene cloning and sequencing. Appl Environ Microbiol **67:** 2932–2941

Falkowski P, Raven JA (1997) Aquatic Photosynthesis. Blackwell Science, Oxford

Finkel ZV (2001) Light absorption and size scaling of light-limited metabolism in marine diatoms. Limnol Oceanogr **46:** 86–94

Forster B, Osmond CB, Pogson BJ (2009) De novo synthesis and degradation of Lx and V cycle pigments during shade and sun acclimation in avocado leaves. Plant Physiol **149:** 1179–1195

Garczarek L, Dufresne A, Blot N, Cockshutt AM, Peyrat A, Campbell DA,

Joubin L, Six C (2008) Function and evolution of the psbA gene family in marine *Synechococcus*: *Synechococcus* sp. WH7803 as a case study. ISME J **2:** 937–953

Gillooly JF, Brown JH, West GB, Savage VM, Charnov EL (2001) Effects of size and temperature on metabolic rate. Science **293:** 2248–2251

Gilmore AM, Yamamoto HY (2001) Time-resolution of the antheraxanthin- and delta pH-dependent chlorophyll *a* fluorescence components associated with photosystem II energy dissipation in *Mantoniella squamata*. Photochem Photobiol **74:** 291–302

Guskov A, Kern J, Gabdulkhakov A, Broser M, Zouni A, Saenger W (2009) Cyanobacterial photosystem II at 2.9-A resolution and the role of quinones, lipids, channels and chloride. Nat Struct Mol Biol **16:** 334–342

Hakala M, Tuominen I, Keranen M, Tyystjarvi T, Tyystjarvi E (2005) Evidence for the role of the oxygen-evolving manganese complex in photoinhibition of photosystem II. Biochim Biophys Acta **1706:** 68–80

Hecks B, Wilhelm C, Trissl HW (1996) Functional organization of the photosynthetic apparatus of the primitive alga *Mantoniella squamata*. Biochim Biophys Acta **1274:** 21–30

Holt NE, Fleming GR, Niyogi KK (2004) Toward an understanding of the mechanism of nonphotochemical quenching in green plants. Biochemistry **43:** 8281–8289

Johnson MP, Davison PA, Ruban AV, Horton P (2008) The xanthophyll cycle pool size controls the kinetics of non-photochemical quenching in *Arabidopsis thaliana*. FEBS Lett **582:** 262–266

Josse EM, Simkin AJ, Gaffe J, Laboure AM, Kuntz M, Carol P (2000) A plastid terminal oxidase associated with carotenoid desaturation during chromoplast differentiation. Plant Physiol **123:** 1427–1436

Keller MD, Selvin RC, Claus W, Guillard RRL (1987) Media for the culture of oceanic ultraphytoplankton. J Phycol **23:** 633–638

Kirk JTO (1976) A theoretical analysis of the contribution of algal cells to the attenuation of light within natural waters. III. Cylindrical and spheroidal cells. New Phytol **77:** 341–358

Krieger-Liszkay A (2005) Singlet oxygen production in photosynthesis. J Exp Bot **56:** 337–346

Krieger-Liszkay A, Fufezan C, Trebst A (2008) Singlet oxygen production in photosystem II and related protection mechanism. Photosynth Res **98:** 551–564

Li XP, Gilmore AM, Caffarri S, Bassi R, Golan T, Kramer D, Niyogi KK (2004) Regulation of photosynthetic light harvesting involves intrathylakoid lumen pH sensing by the PsbS protein. J Biol Chem **279:** 22866–22874

Lovejoy C, Vincent WF, Bonilla S, Roy S, Martineau MJ, Terrado R, Potvin M, Massana R, Pedrós-Alió C (2007) Distribution, phylogeny, and growth of cold-adapted picoprasinophytes in artic seas. J Phycol **43:** 78–89

Matsubara S, Morosinotto T, Osmond CB, Bassi R (2007) Short- and long-term operation of the lutein-epoxide cycle in light-harvesting antenna complexes. Plant Physiol **144:** 926–941

Matsubara S, Naumann M, Martin R, Nichol C, Rascher U, Morosinotto T, Bassi R, Osmond B (2005) Slowly reversible de-epoxidation of lutein-epoxide in deep shade leaves of a tropical tree legume may 'lock-in' lutein-based photoprotection during acclimation to strong light. J Exp Bot **56:** 461–468

Morel A, Bricaud A (1981) Theoretical results concerning light absorption in a discrete medium, and application to specific absorption of phytoplankton. Deep-Sea Res **28:** 1375–1393

Murata N, Takahashi S, Nishiyama Y, Allakhverdiev SI (2007) Photoinhibition of photosystem II under environmental stress. Biochim Biophys Acta **1767:** 414–421

Nagy L, Balint E, Barber J, Ringler A, Cook KM, Maroti P (1995) Photoinhibition and law of reciprocity in photosynthetic reactions of *Synechocystis* sp. PCC 6803. J1. Plant Physiol **145:** 410–444

Nishiyama Y, Allakhverdiev SI, Murata N (2005) Inhibition of the repair of photosystem II by oxidative stress in cyanobacteria. Photosynth Res **84:** 1–7

Nishiyama Y, Allakhverdiev SI, Murata N (2006) A new paradigm for the action of reactive oxygen species in the photoinhibition of photosystem II. Biochim Biophys Acta **1757:** 742–749

Not F, Latasa M, Marie D, Cariou T, Vaulot D, Simon N (2004) A single species, *Micromonas pusilla* (Prasinophyceae), dominates the eukaryotic picoplankton in the western English channel. Appl Environ Microbiol **70:** 4064–4072

Palenik B, Grimwood J, Aerts A, Rouze P, Salamov A, Putnam N, Dupont C, Jorgensen R, Derelle E, Rombauts S, et al (2007) The tiny eukaryote *Ostreococcus* provides genomic insights into the paradox of plankton speciation. Proc Natl Acad Sci USA **104:** 7705–7710

Partensky F, Blanchot J, Lantoine F, Neveux J, Marie D (1996) Vertical structure of picophytoplankton at different trophic sites of the tropical northeastern Atlantic Ocean. Deep-Sea Res I **43:** 1191–1213

Rodriguez F, Chauton M, Johnsen G, Andresen K, Olsen LM, Zapata M (2006) Photoacclimation in phytoplankton: implications for biomass estimates, pigment functionality and chemotaxonomy. Mar Biol **148:** 963–971

Rodríguez F, Derelle E, Guillou L, Le Gall F, Vaulot D, Moreau H (2005) Ecotype diversity in the marine picoeukaryote *Ostreococcus* (Chlorophyta, Prasinophyceae). Environ Microbiol **7:** 853–859

Ruban AV, Berera R, Illioaia C, van Stokkum IHM, Kennis TM, Pascal AA, van Amerongen H, Robert B, Horton P, van Grondelle R (2007) A mechanism of photoprotective energy dissipation in higher plants. Nature **450:** 575–578

Sarvikas P, Hakala M, Patsikka E, Tyystjarvi T, Tyystjarvi E (2006) Action spectrum of photoinhibition in leaves of wild type and npq1-2 and npq4-1 mutants of *Arabidopsis thaliana*. Plant Cell Physiol **47:** 391–400

Silva P, Thompson E, Bailey S, Kruse O, Mullineaux CW, Robinson C, Mann NH, Nixon PJ (2003) FtsH is involved in the early stages of repair of photosystem II in *Synechocystis* sp. PCC 6803. Plant Cell **15:** 2152–2164

Sinclair J, Park YI, Chow WS, Anderson JM (1996) Target theory and the photoinactivation of photosystem II. Photosynth Res **50:** 33–40

Six C, Finkel Z, Rodriguez F, Marie D, Partensky F, Campbell DA (2008) Contrasting photoacclimatation costs in ecotypes of the marine picoplankter *Ostreococcus*. Limnol Oceanogr **53:** 255–265

Six C, Finkel ZV, Irwin AJ, Campbell DA (2007) Light variability illuminates niche-partitioning among marine picocyanobacteria. PLoS One **2:** e1341

Six C, Worden AZ, Rodriguez F, Moreau H, Partensky F (2005) New insights into the nature and phylogeny of prasinophyte antenna proteins: *Ostreococcus tauri*, a case study. Mol Biol Evol **22:** 2217–2230

Stirbet A, Govindjee, Strasser BJ, Strasser RJ (1998) Chlorophyll a fluorescence induction in higher plants: modelling and numerical simulation. J Theor Biol **193:** 131–151

Telfer A (2005) Too much light? How beta-carotene protects the photosystem II reaction centre. Photochem Photobiol Sci **4:** 950–956

Turmel M, Gagnon MC, O'Kelly CJ, Otis C, Lemieux C (2009) The chloroplast genomes of the green algae *Pyramimonas*, *Monomastix*, and *Pycnococcus* shed new light on the evolutionary history of prasinophytes and the origin of the secondary chloroplasts of euglenids. Mol Biol Evol **26:** 631–648

Tyystjarvi E (2008) Photoinhibition of photosystem II and photodamage of the oxygen evolving manganese cluster. Coord Chem Rev **252:** 361–376

Tyystjarvi E, Aro EM (1996) The rate constant of photoinhibition, measured in lincomycin-treated leaves, is directly proportional to light intensity. Proc Natl Acad Sci USA **93:** 2213–2218

Vankooten O, Snel JFH (1990) The use of chlorophyll fluorescence nomenclature in plant stress physiology. Photosynth Res **25:** 147–150

Zapata M, Rodriguez F, Garrido JL (2000) Separation of chlorophylls and carotenoids from marine phytoplankton: a new HPLC method using a reversed phase C-8 column and pyridine-containing mobile phases. Mar Ecol Prog Ser **195:** 29–45

Zhu F, Massana R, Not F, Marie D, Vaulot D (2005) Mapping of picoeucaryotes in marine ecosystems with quantitative PCR of the 18S rRNA gene. FEMS Microbiol Ecol **52:** 79–92